Chemistry–A European Journal
Research Article
doi.org/10.1002/chem.202400820
Chemistry Europe
European Chemical Societies Publishing
www.chemeurj.org

Wavelength-Dependent Activation of Photoacids and Bases

Petra Utroša,[c] Joshua A. Carroll,[a] Ema Žagar,[c] David Pahovnik,[c] and Christopher Barner-Kowollik*[a, b]

Photoacids and bases allow remote control over pH in reaction solutions, which is of fundamental importance to an array of applications. Herein, we determine the wavelength-by-wavelength resolved photoreactivity of triarylsulfonium hexafluorophosphate salts as a representative photoacid generator and *p*-(benzoyl)benzyl triethylammonium tetraphenylborate as a photobase generator, constructing a wavelength-resolved photochemical action plot for each of the compounds. We monitor the pH change of the solution on-line within the cavity of the laser vial and demonstrate a marked mismatch between the absorption spectrum of the photoacid and base with the photochemical action plot, unveiling reactivity at very low absorptivities. Our findings are of critical importance for the use of photoacids and bases, unambiguously demonstrating that absorption is no guide to chemical reactivity with critical consequences for the wavelength employed in applications of photoacids and bases.

Introduction

Changing pH is fundamental to drive numerous chemical, material, and biological processes. Currently, photochemistry is undergoing a precision revolution as a finely energy-gated synthetic tool using photons as a traceless reagent, enabling remote control over when and where reactions occur, including within a molecule.[1] Proton transfer can be photochemically controlled[2] using photoacids as photoreactive compounds that generate a Brønsted acid upon irradiation; and, analogously, photobases that photogenerate basic species.[3] Photoacid and base generators, which undergo irreversible structural changes upon irradiation, have been strongly explored in the field of polymer science with the aim of inducing photopolymerization[3a,4] or causing a change in the physical properties of a polymer.[5] Photoacids have also emerged as valuable catalysts in organic synthesis,[6] and their applicability has been extended to various biomedical applications.[7]

Selecting the ideal irradiation wavelength is critical to achieve sufficient penetration depth of light, minimize side reactions or tissue damage caused by high-energy light sources, and to manipulate distinct photochemical processes independently of each other (i.e., wavelength-orthogonally).[7,8] Complementary to the careful structural design of a chromophore,[9] studying its wavelength-by-wavelength response to photons has emerged as a critical parameter, most notably in the form of photochemical action plots introduced by our team.[1b,10] Wavelength-tuneable optical parametric oscillators–in the following referred to as lasers–have been employed to investigate the reactivities of various photochemical processes with monochromatic wavelength resolution via our photochemical action plot methodology.[1b,11] Photochemical action plot analysis provides key insight into photoreactivity, and we have revealed a strong red-shift in efficiency of the photochemical process relative to the absorption maximum well into regions of very low absorptivity, illustrating a mismatch between absorptivity and photochemical reactivity for several reactions.[11] Specifically, photoreactivity is analysed by directly quantifying the conversion to photoproducts via spectrophotometry,[12] NMR spectroscopy,[13] and mass spectrometry,[14] or by indirectly following a secondary change triggered by the photoreaction (e.g. conversion during free-radical polymerization induced by photodecomposition of a photoinitiator).[10,15] The above analyses are typically conducted off-line by post-irradiation characterization. However, it is highly attractive to monitor the photochemical response within the laser vial, which is particularly critical when photogenerated products reverse to starting compounds in the absence of light or for highly sensitive products that may react further.

Measuring the pH of reaction solutions presents a simple approach for the evaluation of proton transfer reactions, allowing rapid analysis with no need for deuterated solvents and no further sample preparation. Herein, we monitor the photoactivation of irreversible activation of a photoacid and base under irradiation with monochromatic wavelengths via a change in the pH value of the reaction solution (Figure 1). We thus introduce pH-based photochemical action plots, using a triarylsulfonium hexafluorophosphate salt mixture as a repre-

[a] J. A. Carroll, C. Barner-Kowollik
Centre for Materials Science, School of Chemistry and Physics, Queensland University of Technology (QUT), 2 George Street, QLD 4000 Brisbane, Australia
E-mail: christopher.barnerkowollik@qut.edu.au
[b] C. Barner-Kowollik
Institute of Nanotechnology (INT), Karlsruhe Institute of Technology (KIT), Hermann-von-Helmholtz-Platz 1, 76344 Eggenstein-Leopoldshafen, Germany
E-mail: christopher.barner-kowollik@kit.edu
[c] P. Utroša, E. Žagar, D. Pahovnik
Department of Polymer Chemistry and Technology, National Institute of Chemistry, Hajdrihova 19, 1000 Ljubljana, Slovenia

Supporting information for this article is available on the WWW under https://doi.org/10.1002/chem.202400820

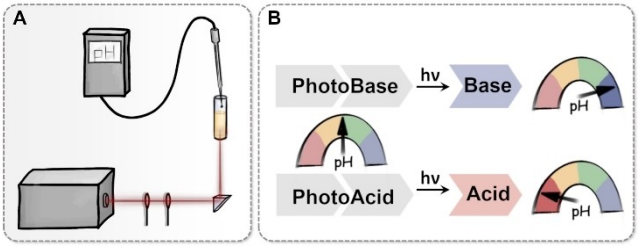

Figure 1. (A) Schematic representation of the pH photochemical action plot set-up used for conducting irradiation experiments, utilizing a wavelength-tuneable laser and a pH meter. (B) Photodecomposition of a photobase is observed by an increase in pH, and photodecomposition of a photoacid leads to pH decrease.

sentative photoacid, and *p*-(benzoyl)benzyl triethylammonium tetraphenylborate as an example of a photobase.

Results and Discussion

Water is the most appropriate solvent to measure pH, as H^+ activity in aqueous solutions defines the familiar pH scale (0–14).[16] However, many photoacids and photobases, including triarylsulfonium hexafluorophosphate salts and *p*-(benzoyl)benzyl triethylammonium tetraphenylborate, have low solubility in water. pH sensors may face precipitation of the reference electrolyte when immersed in organic solvent, as they are not designed for measuring non-aqueous solutions.[17] Herein, we use acetonitrile as a suitable solvent for the photoacid and base and mix it with water to avoid pH sensor malfunction, while still being able to prepare 1 mM solutions in water/acetonitrile in a 5:4 volume ratio. pH as a function of acid or base concentration in water/acetonitrile (5:4) solvent mixture exhibits lower pH values compared to expected pH in water, yet follows a linear trend (Figure S4). It should be noted that the absolute pH scale of any organic solvent or its mixture deviates from the familiar pH scale.[16]

Triarylsulfonium salts bearing weakly coordinating anions (e.g. hexafluorophosphate, PF_6^-) generate a Brønsted acid (e.g. hexafluorophosphoric acid, HPF_6) as a result of irreversible photolysis under irradiation (Figure 2A).[18] Light promotes tetraphenylsulfonium to a singlet excited state, which results in the cleavage of the S–C bond, followed by the formation of intermediate radicals. Subsequent radical-radical combinations and radical-photoproduct addition reactions occur, the result of which are multiple aromatic by-products.[18b] Interestingly, while the triarylsulfonium hexafluorophosphate salts photoacid exhibits its maximal absorption at $\lambda = 296$ nm, it has generally been irradiated with broad-band light sources with a peak maximum at 365 nm to initiate cationic polymerization.[19] Herein, we irradiated a solution of triarylsulfonium hexafluorophosphate photoacid (1 mM in water/acetonitrile 5:4) with monochromatic light, employing a tuneable nanosecond pulsed laser system. Structural characterization of the photoproducts after 10 min of irradiation at 365 nm (correlating to $3.73 \cdot 10^{18}$ photons at incident beam energy of 200 μJ) via ^{1}H NMR spectroscopy

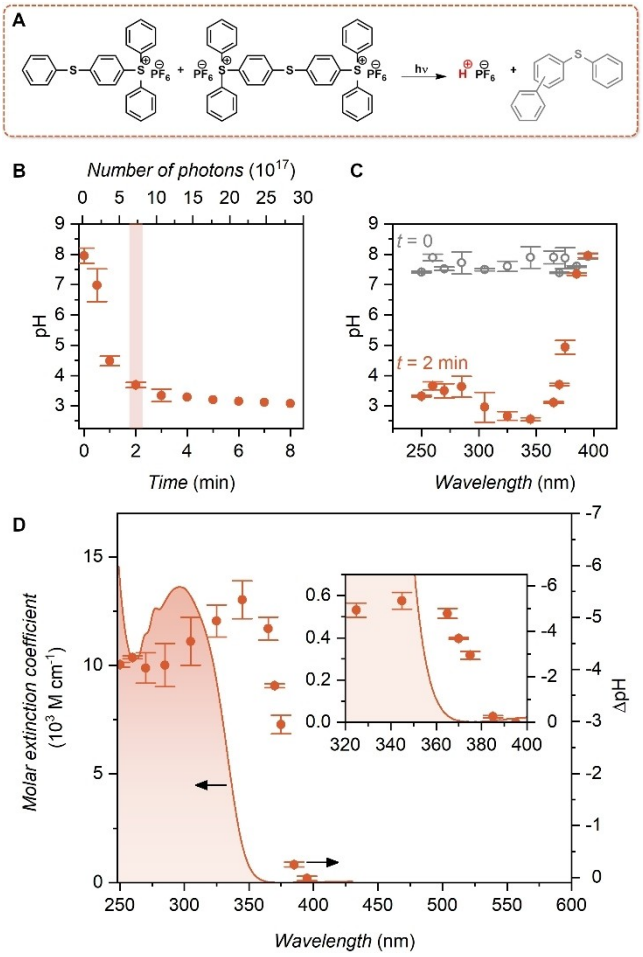

Figure 2. (A) Proposed reaction of triarylsulfonium hexafluorophosphate salts photoacid upon irradiation, resulting in the photogeneration of hexafluorophosphoric acid and aromatic by-products. (B) Recorded pH of the photoacid solution (1 mM in water/acetonitrile 5:4) as a function of time/number of photons during irradiation with monochromatic light at 365 nm with an incident beam of 200 μJ. (C) Recorded pH of the photoacid solution (1 mM in water/acetonitrile 5:4) before and after irradiation for 2 min at fixed number of photons ($7.46 \cdot 10^{17}$) as a function of wavelength. (D) Photochemical action plot of the photoacid, depicting the absorption spectrum and the change in pH of the reaction solution as a function of wavelength.

shows the appearance of new aromatic resonances (Figure S5), corresponding to the radical-mediated photoproducts.[18b,20] ^{19}F (Figure S6) and ^{31}P (Figure S7) NMR spectra reveal no information regarding the anionic part of the photoacid, as no change in chemical shift is observed in the photoacid before irradiation and the proposed acid after irradiation. However, the pH of the same irradiated photoacid solution decreased by 5.2 units in water/acetonitrile 5:4, revealing the acid photorelease at 365 nm (Figure 2B) that could otherwise have been missed when relying only on NMR. Based on the time-dependent pH monitoring, the 2 min time point was used to determine the number of photons ($7.46 \cdot 10^{17}$) for mapping the photoacid photochemical reactivity in terms of pH change at different wavelengths, ranging from 250 nm to 395 nm (Figure 2C and D, Table S1). Sufficiently low conversion to photoproducts is required to obtain a reliable photochemical action plot,

otherwise near full conversion is reached at different wavelengths and the photoreactivity maximum is not well resolved (Figure S8). Notably, the pH of the photoacid solution kept in the dark remained constant over time (Figure S9), confirming that the reaction at room temperature can only proceed photochemically. A control experiment using a blank solvent sample irradiated with the same number of photons ($7.46 \cdot 10^{17}$) over the wavelength range resulted in no pH change, confirming that the photoacid is critical for the proton transfer (Figure S10). The pH change of the 1 mM photoacid solution reached its maximum at 345 nm, which is more than 40 nm red-shifted compared to the absorptivity maximum ($\lambda =$ 296 nm), tailing to 385 nm, where the absorptivity approaches already nearly zero. A mismatch between absorptivity and reactivity has been observed for a large number of investigated photoreactive chromophores and may stem – among other potential factors – from the fact that the absorption spectrum of a chromophore typically does not contain information about excited state dynamics that plays a critical role in determining the energy redistribution after photon absorption.[1b,11] The remarkable red-shift in photoreactivity of the photoacid under investigation appears to be even more pronounced at a higher concentration (10 mM in water/acetonitrile 5:4) at the same number of photons (Figure S11).

We subsequently mapped the photoreactivity of the tetraphenylborate photobase in a similar manner. The absorption spectrum of the photobase in water/acetonitrile (5:4) is characterized by a strong π-π* transition peak in the low wavelengths region (230–300 nm) and a weak band centred at 325 nm corresponding to a n-π* transition of the benzophenone moiety.[21] It has been proposed that the n-π* transition allows for the decomposition of this type of photobase using a 300–400 nm mercury lamp, irreversibly liberating free triethylamine by benzophenone triplet state oxidation of the borate followed by C–N bond cleavage (Figure 3A).[21a,22] We irradiated the 1 mM photobase solution with a monochromatic light at $\lambda = 365$ nm (120 μJ incident beam energy), and observed a noticeable increase in pH value over 10 min time (Figure 3B). pH of the irradiated photobase starts to level off at ΔpH~2, since triethylamine is a weak base. We kept the number of photons constant at $3.59 \cdot 10^{17}$ (corresponding to 2 min irradiation time) to scan the photoreactivity within the 250–385 nm wavelength range (Figure 3C), in order to avoid a cut-off of the ΔpH peak (Figure S12). The photoinduced pH change peak is clearly visible in the action plot at $\lambda = 325$ nm, overlapping with the weak n-π* transition seen in the absorption spectrum (Figure 3D). The reactivity of the photobase expands up to 375 nm despite a significant decrease in absorptivity.

While there is a prominent change in the pH value of the photobase solution irradiated for 2 min at 325 nm, triethylamine release is not well resolved in the ^{1}H NMR spectra (Figure S13). Protons corresponding to methyl groups of the photobase feature a resonance at 1.35 ppm, while free triethylamine should exhibit the corresponding methyl proton resonances at 0.95 ppm. As the photobase is irradiated further and the solution pH decreases for 2.8 units after 5 min, a new resonance at 1.11 ppm is observed due to the photogenerated

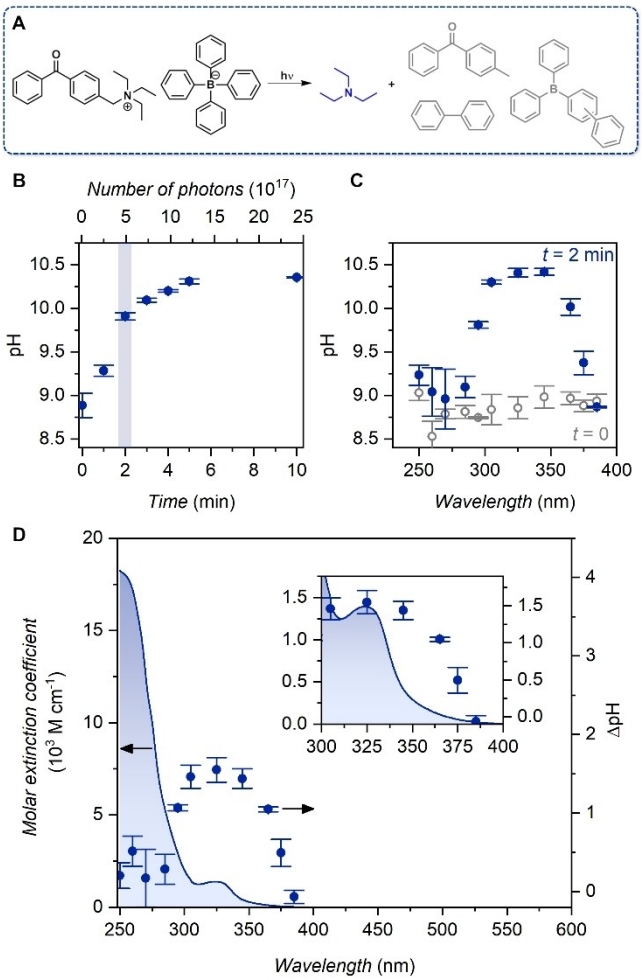

Figure 3. (A) Proposed reaction of *p*-(benzoyl)benzyl triethylammonium tetraphenylborate photobase upon irradiation, resulting in the photogeneration of triethylamine, triphenylborane, and aromatic by-products. (B) Recorded pH of the photobase solution (1 mM in water/acetonitrile 5:4) as a function of time/number of photons during irradiation with monochromatic light at 365 nm with an incident beam of 120 μJ. (C) Recorded pH of the photobase solution (1 mM in water/acetonitrile 5:4) before and after irradiation for 2 min at a fixed number of photons ($3.59 \cdot 10^{17}$) as a function of wavelength. (D) Photochemical action plot of the photobase, depicting the absorption spectrum and the change in pH of the reaction solution as a function of wavelength.

triethylamine. The signal is shifted downfield compared to free triethylamine, as the nitrogen lone-pair electrons interact with an unoccupied p-orbital of boron in the triphenylborane photoproduct.[23] Compared to pH measurements, the amine photorelease may be concealed in ^{1}H NMR spectra due to the nitrogen–boron interactions. In the case of the studied photobase, measuring the pH change again proved to be extremely beneficial to follow photoreactivity and obtain the action plot.

Conclusions

We introduce the wavelength-by-wavelength resolved photoreactivity of a photoacid and a base in a simple and facile manner via pH monitoring, which proves to be suitable for

following photogeneration of acids as well as bases, with no need for additional sample preparation or use of deuterated solvents. The reported method for obtaining photochemical action plots is particularly advantageous where typical characterization methods (e.g. spectrophotometry, NMR spectroscopy) fail to unambiguously confirm the proton transfer reaction. These on-line measurements also allow for the characterisation of certain reaction intermediates, or for products that thermally revert to starting materials. We observe a strong mismatch between the absorption spectrum and the photochemical reactivity of the photoreactive acid and base, with critical consequences for their use in synthetic applications. We submit that each photoacid or base must be assessed via a photochemical action plot to determine its optimum and mildest reactivity range, as absorption spectra fail to predict the photochemical reactivity.

Experimental Section

Characterization

^{1}H (600.13 MHz), ^{19}F (564.69 MHz) and ^{31}P (242.94 MHz) NMR spectra were recorded on a Bruker System 600 Ascend LH. Solution absorption spectra were recorded on a Shimadzu UV-2700 spectrophotometer equipped with a temperature control cell positioner. Samples were measured in quartz cuvettes at 25 °C. pH was measured using a MI-410 micro-combination pH microelectrode and a WP-90 pH meter. The pH electrode was calibrated in aqueous buffers (pH values 4.01, 7.00, and 10.01). For measurements in water/acetonitrile mixture, an equilibration time was allowed for pH readout to reach a constant value (< 2 min). The pH electrode was immersed in deionized water in between non-aqueous measurements.

Materials

Acetonitrile, 4-(bromomethyl)benzophenone, sodium tetraphenylborate, triethylamine, and trifluoroacetic acid (TFA) were obtained from Sigma Aldrich; diethyl ether and triarylsulfonium hexafluorophosphate salts (mixed, 50% in propylene carbonate) were obtained from Merck, while acetone and chloroform were obtained from Honeywell, and ethanol from Carlo Erba. All chemicals and solvents were used as received.

p-(Benzoyl)benzyl Triethylammonium Tetraphenylborate Photobase Synthesis

The photobase was synthesised based on a previously reported procedure.[21a] Briefly, triethylamine (2.07 mL, 14.8 mmol) was slowly added to 4-(bromomethyl)benzophenone (3.40 g, 12.4 mmol) dissolved in chloroform/diethyl ether 1:1 (v/v, 60 mL) and left to stir at room temperature for 24 h, upon which the reaction mixture split into two phases. We separated the bottom phase and dried it under vacuo. The solid residue was recrystallized from acetone and dried under vacuo to obtain *p*-(benzoyl)benzyl triethylammonium bromide (3.46 g, 9.2 mmol, 74% yield). The *p*-(benzoyl)benzyl triethylammonium bromide was dissolved in deionised water (14 mL) and filtered to remove any insoluble impurities. A solution of sodium tetraphenylborate (3.14 g, 9.2 mmol) in deionised water (12 mL) was slowly added, upon which a precipitate formed. The precipitate was isolated by centrifugation (7,500 rpm, 5 min) and dried under vacuo, followed by recrystallization from ethanol/acetonitrile to obtain *p*-(benzoyl)benzyl triethylammonium tetraphenylborate as white needle-like crystals (4.77 g, 63% yield). ^{1}H NMR (DMSO-d_6, 600 MHz, δ (ppm)): 7.81 (m, 4H, *ortho* to carbonyl), 7.75–7.55 (m, 5H, *meta* and *para* to carbonyl), 7.17 (m, 8H, *ortho* to B), 6.92 (t, 8H, *meta* to B), 6.78 (t, 4H, *para* to B), 4.58 (s, 2H, Ar-CH_2–), 3.21 (q, 6H, –N–CH_2–), 1.33 (t, 9 H, –N–CH_2–CH_3).

Photoreactivity Experiments[1b]

Irradiation experiments were conducted using a nanosecond pulsed, tuneable optical parametric oscillator laser Opotek Opolette 355. Stock solutions were prepared by dissolving the photoacid or the photobase in a mixture of water and acetonitrile in 5:4 volume ratio. Deuterated solvents (D_2O and acetonitrile-d_3) were used for samples that were further analysed by NMR spectroscopy. Samples were prepared by transferring stock solution (500 μL) into (quartz) glass crimp neck vials (8 mm diameter, flat bottom), stopped with rubber septum and kept in dark until measurement. Sample conditions are listed in Table S1. The laser beam was passed through a beam expander (−50 mm and 100 mm lens combination) and collimated, then directed upwards using a UV silica right angle prism used as a mirror. The beam entered the bottom of the sample vial held in an aluminium block. The pH of the reaction solution was measured after specified irradiation time by inserting the microelectrode pH probe directly in the laser vial. The energy of the beam was measured above the aluminium block before and after experiments using a Coherent EnergyMax thermopile sensor (J–25 MB–LE).

Supporting Information Summary

The data that support the findings of this study are available in the Supporting Information of this article.

Acknowledgements

P.U. acknowledges financial support from the Slovenian Research and Innovation Agency (Research Core Funding No. P2-0145 and project No. Z2-4439). C.B.-K. acknowledges the Australian Research Council (ARC) for funding in the context of a Laureate Fellowship enabling his photochemical research program and continued support by QUT Centre for Materials Science. The Central Analytical Research Facility (CARF) at QUT is gratefully acknowledged. Open Access publishing facilitated by Queensland University of Technology, as part of the Wiley - Queensland University of Technology agreement via the Council of Australian University Librarians.

Conflict of Interests

The authors declare no conflict of interest.

Data Availability Statement

The data that support the findings of this study are available in the supplementary material of this article.

Keywords: Photoacids · Photobases · pH Control · Action plot analysis

[1] a) P. Lu, D. Ahn, R. Yunis, L. Delafresnaye, N. Corrigan, C. Boyer, C. Barner-Kowollik, Z. A. Page, *Matter* **2021**, *4*, 2172–2229; b) I. M. Irshadeen, S. L. Walden, M. Wegener, V. X. Truong, H. Frisch, J. P. Blinco, C. Barner-Kowollik, *J. Am. Chem. Soc.* **2021**, *143*, 21113–21126.
[2] a) L. Wimberger, S. K. K. Prasad, M. D. Peeks, J. Andréasson, T. W. Schmidt, J. E. Beves, *J. Am. Chem. Soc.* **2021**, *143*, 20758–20768; b) L. Wimberger, J. Andréasson, J. E. Beves, *Chem. Commun.* **2022**, *58*, 5610–5613; c) A. Yucknovsky, Y. Shlosberg, N. Adir, N. Amdursky, *Angew. Chem. Int. Ed.* **2023**, *62*, e202301541.
[3] a) N. Zivic, P. K. Kuroishi, F. Dumur, D. Gigmes, A. P. Dove, H. Sardon, *Angew. Chem. Int. Ed.* **2019**, *58*, 10410–10422; b) Y. Liao, *Phys. Chem. Chem. Phys.* **2022**, *24*, 4116–4124.
[4] K. Suyama, M. Shirai, *Prog. Polym. Sci.* **2009**, *34*, 194–209.
[5] W. Alabiso, Y. Li, J. Brancart, G. Van Assche, E. Rossegger, S. Schlögl, *Polym. Chem.* **2024**, *15*, 321–331.
[6] J. Saway, Z. M. Salem, J. J. Badillo, *Synthesis* **2021**, *53*, 489–497.
[7] T. Sun, L. Kang, H. Zhao, Y. Zhao, Y. Gu, *Adv. Sci.* **2023**, *11*, 2302875.
[8] J. T. Offenloch, M. Gernhardt, J. P. Blinco, H. Frisch, H. Mutlu, C. Barner-Kowollik, *Chem. – Eur. J.* **2019**, *25*, 3700–3709.
[9] P. Štacko, T. Šolomek, *CHIMIA* **2021**, *75*, 873–881.
[10] D. E. Fast, A. Lauer, J. P. Menzel, A.-M. Kelterer, G. Gescheidt, C. Barner-Kowollik, *Macromolecules* **2017**, *50*, 1815–1823.
[11] S. L. Walden, J. A. Carroll, A. Unterreiner, C. Barner-Kowollik, *Adv. Sci.* **2023**, *11*, 2306014.
[12] I. M. Irshadeen, V. X. Truong, H. Frisch, C. Barner-Kowollik, *Chem. Commun.* **2023**, *59*, 11959–11962.
[13] D. E. Marschner, H. Frisch, J. T. Offenloch, B. T. Tuten, C. R. Becer, A. Walther, A. S. Goldmann, P. Tzvetkova, C. Barner-Kowollik, *Macromolecules* **2018**, *51*, 3802–3807.
[14] F. Feist, J. P. Menzel, T. Weil, J. P. Blinco, C. Barner-Kowollik, *J. Am. Chem. Soc.* **2018**, *140*, 11848–11854.
[15] P. Neidinger, J. Davis, J. A. Carroll, J. Kammerer, E. Jaatinen, S. L. Walden, A.-N. Unterreiner, C. Barner-Kowollik, *Polym. Chem.* **2023**, *14*, 4912–4917.
[16] D. Himmel, S. K. Goll, I. Leito, I. Krossing, *Angew. Chem. Int. Ed.* **2010**, *49*, 6885–6888.
[17] A. Heering, F. Bastkowski, S. Seitz, *J. Sens. Sens. Syst.* **2020**, *9*, 383–389.
[18] a) A. Chemtob, C. Belon, C. Croutxé-Barghorn, S. Rigolet, L. Vidal, J. Brendlé, J. Mandel, N. Blanchard, *Polym. Eng. Sci.* **2011**, *51*, 1466–1475; b) J. V. Crivello, *J. Polym. Sci. Part Polym. Chem.* **1999**, *37*, 4241–4254.
[19] a) I. A. Barker, A. P. Dove, *Chem. Commun.* **2013**, *49*, 1205–1207; b) M. Li, L. Zhou, Z. Zhang, Q. Wang, J. Gao, S. Zhang, L. Lei, *Polym. Chem.* **2021**, *12*, 5069–5076.
[20] X.-Z. Niu, R. D. Pepel, R. Paniego, J. A. Field, J. Chorover, L. Abrell, A. E. Sáez, R. Sierra-Alvarez, *J. Photochem. Photobiol. Chem.* **2021**, *416*, 113324.
[21] a) A. M. Sarker, A. Lungu, A. Mejiritski, Y. Kaneko, D. C. Neckers, *J. Chem. Soc. Perkin Trans* **1998**, *2*, 2315–2322;b) A. Mejiritski, A. Y. Polykarpov, A. M. Sarker, D. C. Neckers, *Chem. Mater.* **1996**, *8*, 1360–1362.
[22] A. M. Sarker, Y. Kaneko, A. V. Nikolaitchik, D. C. Neckers, *J. Phys. Chem. A* **1998**, *102*, 5375–5382.
[23] a) W. Zhang, K. Feng, X. Wu, D. Martin, D. C. Neckers, *J. Org. Chem.* **1999**, *64*, 458–463; b) M. F. Sonnenschein, S. P. Webb, O. D. Redwine, B. L. Wendt, N. G. Rondan, *Macromolecules* **2006**, *39*, 2507–2513.

Manuscript received: February 28, 2024
Accepted manuscript online: April 29, 2024
Version of record online: May 17, 2024